
# The effect of sample resistivity on Kelvin probe force microscopy

A. J. Weymouth and F. J. Giessibl

Citation: Applied Physics Letters **101**, 213105 (2012); doi: 10.1063/1.4766185

View online: http://dx.doi.org/10.1063/1.4766185

View Table of Contents: http://scitation.aip.org/content/aip/journal/apl/101/21?ver=pdfcov

Published by the AIP Publishing



# The effect of sample resistivity on Kelvin probe force microscopy

A. J. Weymouth and F. J. Giessibl
*Institute of Experimental and Applied Physics, University of Regensburg, 93040 Regensburg, Germany*

(Received 14 September 2012; accepted 22 October 2012; published online 21 November 2012)

Kelvin probe force microscopy (KPFM) is a powerful technique to probe the local electronic structure of materials with atomic force microscopy. One assumption often made is that the applied bias drops fully in the tip-sample junction. We have recently identified an effect, the Phantom force, which can be explained by an ohmic voltage drop near the tip-sample junction causing a reduction of the electrostatic attraction when a tunneling current is present. Here, we demonstrate the strong effect of the Phantom force upon KPFM that can even produce Kelvin parabolae of opposite curvature. © *2012 American Institute of Physics*. [http://dx.doi.org/10.1063/1.4766185]

Kelvin probe force microscopy (KPFM) is an atomic force microscopy (AFM) technique to probe the local contact potential difference ($V_{CPD}$) of a sample.[1] As the attractive force between tip and sample is related to the potential drop in the tip-sample junction, $V_{CPD}$ can be determined by adjusting the applied bias voltage. However, if this induces a tunneling current, then ohmic effects outside the junction can affect measurements. We have recently reported upon a Phantom force that can dominate AFM images, in which attractive surface features can appear relatively repulsive.[2,3] In this letter, we describe the effect of the Phantom force upon KPFM.

KPFM is used to measure the local work function of a material. It is based upon the principle that two surfaces with different work functions, for example, $\phi_1$ and $\phi_2$, have a contact potential difference between them of $V_{CPD} = (\phi_2 - \phi_1)/e$, where $e$ is the elementary charge, in addition to any applied bias. As the attractive force in a capacitive junction, such as that between a metallic probe tip and sample, is a function of the total potential drop in that junction, $V_{CPD}$ can be determined by measuring the force as a function of the applied bias.

The interpretation of KPFM data, however, is not necessarily straightforward.[4] Over insulating substrates,[5] the dielectric layer must be considered and complicates interpretation.[6] Even when thin insulating layers are used to decouple systems and produce impressive KPFM results,[7,8] the effect of the insulating layer cannot be ignored.[9] On some semiconductor surfaces, it has been shown that the effect of a dielectric, most often considered in the framework of tip-induced band bending, can be neglected.[10] However, it has been reported that at close tip-sample distances, the interaction of the tip and sample wavefunctions can apparently change the local $V_{CPD}$.[11]

The most common non-contact AFM technique is frequency-modulation AFM (FM-AFM), in which the tip is oscillated on a cantilever with spring constant $k$ at a resonance frequency $f_0$.[12] This method allows a measure of the force gradient, $k_{ts} = -\mathrm{d}F/\mathrm{d}z$, weighted over the oscillation of the tip, where $F$ is the component of force normal to the sample surface. The interaction between the tip and surface is measured by the frequency shift $\Delta f$ which is related to $k_{ts}$

$$\Delta f = \frac{f_0}{2k}\langle k_{ts}\rangle, \tag{1}$$

where the brackets around $k_{ts}$ denote the weighted average of $k_{ts}$ (see, e.g., Ref. 13, for details). Important here is that FM-AFM does not probe the force between the tip and sample but rather the averaged force gradient.

We have recently reported upon a phenomenon that can dominate AFM images when a tunneling current is present. We have explained this by a local ohmic voltage drop within the sample near the tip-sample junction, that can be described by a resistance $R_S$. Ohmic resistive drops have been used to explain energy shifts in tunneling spectroscopy[14] and there is increasing evidence that they can be dominated by local effects near the tip-sample junction.[3,15] While our initial explanation described the voltage drop only within the sample, this voltage drop can also occur in the tip, as demonstrated in Ref. 15. As the tunneling current increases, the voltage drop across $R_S$ increases and as a consequence, the potential difference of the tip-sample junction decreases. This in turn causes a decrease of the electrostatic force $F^{es}$, the effect of which is that attractive sites on the surface display a positive average force gradient such that they can appear repulsive. We call this effect the Phantom force. While our data were collected with a qPlus AFM sensor, the Phantom force has been recently reported by combined AFM/STM with commercial Pt/Ir-coated Si cantilevers.[16]

Considering just the attractive electrostatic force between tip and sample, the force on the tip is a function of the electrostatic field of the sample. This can be written as a function of the capacitance, $C$, the tip-sample distance $z$, and the voltage between tip and sample, $V_J$

$$F^{es} = \frac{1}{2}\frac{\mathrm{d}C}{\mathrm{d}z}V_J^2. \tag{2}$$

For the case of a sphere of radius $\mathcal{R}$ in front of a plate, a good approximation of $F^{es}$ is given by Ref. 17

$$F^{es} = -\pi\epsilon_0 V_J^2 \frac{\mathcal{R}^2}{z(z+\mathcal{R})}. \tag{3}$$

 

Here, $z$ is the closest distance between the sphere and plate and $\epsilon_0$ is the electric constant.

To consider the effect of the Phantom force upon KPFM, we evaluate the effect of $R_S$ upon the voltage drop in the tip-sample junction

$$V_J = V_B \frac{R_J}{R_J + R_S} + V_{CPD}, \tag{4}$$

where $R_J$ is the resistance of the tip-sample junction, and $V_B$ is the applied bias voltage. As $R_J$ is nominally considered to be exponential, it can be expressed as $R_J = R_0 \exp[2\kappa z]$, where $R_0$ is the point-contact resistance, which would be ideally the reciprocal of the quantum point contact conductance, $1/G_0 = h/(2e^2) \approx 12.9\,\mathrm{k\Omega}$, and where $\kappa$ is the decay constant. Schematically, the overall model is shown in Fig. 1(a). $V_J$ is no longer independent of $z$, and so the force gradient of $F^{es}$ now has two terms, the first with the second derivative of capacitance, and the second with the derivative of $V_J$

$$k_{ts}^{es} = \frac{1}{2}\frac{\mathrm{d}^2 C}{\mathrm{d}z^2} V_J^2 + \frac{\mathrm{d}C}{\mathrm{d}z} V_J \frac{\mathrm{d}V_J}{\mathrm{d}z}. \tag{5}$$

In the case of the sphere-plate model in Eq. (3)

$$k_{ts}^{es} = -\epsilon_0 \pi \left[ \frac{\mathcal{R}^2}{z^2(z+\mathcal{R})} + \frac{\mathcal{R}^2}{z(z+\mathcal{R})^2} \right] V_J^2 + 2\pi\epsilon_0 \frac{\mathcal{R}^2}{z(z+\mathcal{R})} \frac{2\kappa e^{2\kappa z} R_S R_0}{(R_0 e^{2\kappa z} + R_S)^2} V_J V_B. \tag{6}$$

The first term is the normal term when considering KPFM. In the case where $R_S$ is zero, $V_J$ reduces to $V_J = V_B + V_{CPD}$, and the second term in Eqs. (5) and (6) reduces to zero. This describes the normal Kelvin parabola, where $\Delta f$ is parabolic as a function of $V_B$ with negative curvature, centred at $-V_{CPD}$. It is easier to see why the second term reduces to zero with $R_S = 0$ when examining Eq. (5) and looking at Fig. 1(a): $V_B$ would drop fully across $R_J$ independently of $z$, meaning that $(\mathrm{d}V_J/\mathrm{d}z) = (\mathrm{d}V_B/\mathrm{d}z) = 0$.

It is important to comment on why we started from Eq. (2) instead of deriving force from the electrostatic potential energy stored in the capacitive junction, $U^{es} = \frac{1}{2} C V_J^2$. First, it can be shown that Eq. (2) is correct from first principles for a parallel-plate model. Taking the plates to have charge density $\sigma$ and $-\sigma$ leads to each plate generating an electric field with magnitude $E = \sigma/(2\epsilon_0)$. The force per area on one plate is $\mathrm{d}F = \sigma(\sigma/(2\epsilon_0))$ making the total force on that plate $F = A(\sigma^2/(2\epsilon_0))$. The voltage between the two is a function of the total electric field between the two plates, $V = (z\sigma)/(\epsilon_0)$, such that $F = \frac{1}{2}\epsilon_0 V^2 (A/z^2)$. For a parallel-plate capacitor with $C = \epsilon_0 (A/z)$, Eq. (2) describes the attractive force. In this case, $F^{es}$ is not simply proportional to the spatial derivative of $U^{es}$ because the applied bias can supply work to the system. In other words, $U^{es}$ is not a complete description of the potential energy of the system because the system is not closed energetically: The work that is done by the tunneling current sourced by the tunneling bias is not included in $U^{es}$.

The two terms in Eqs. (5) and (6) are of opposite sign. This can be seen when evaluating Eq. (5), for a specific case, as is shown in Eq. (6). For certain parameters, $k_{ts}^{es}$ can be positive.

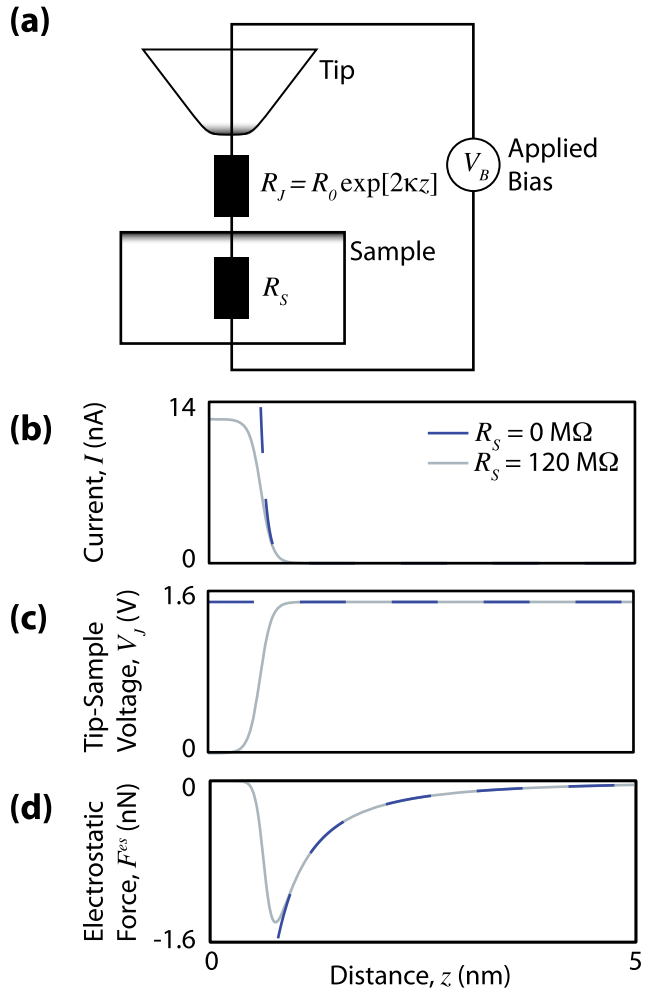


FIG. 1. (a) Schematic view of the probe tip, the junction, and the sample. The applied bias $V_B$ drops in two steps: first, across the junction $R_J$ with a voltage step $R_J I$ and second, across the sample with a voltage step $R_S I$. (b) One effect of this $R_S$ term is that the maximum current decreases. (c) As $R_S \gg R_J$, the voltage difference between the tip and sample vanishes and thus (d) the attractive force on the tip decreases to zero. Here, $R_S = 120\,\mathrm{M\Omega}$, $R_0 = 12.3\,\mathrm{k\Omega}$, $V_b = 1.5\,\mathrm{V}$, $\kappa = 0.8 \times 10^{10}\,\mathrm{m}^{-1}$, and $A = (5\,\mathrm{nm})^2$.

One prediction of this model is that the tunneling current does not increase exponentially as the tip approaches the sample, but is limited as shown in Fig. 1(b). Non-exponential behaviour in the tunneling current has been observed before and another physical explanation is that the electronic states of the tip can, in certain cases, deplete the local density of states of the probed surface atom.[18]

The effect of $R_S$ on $V_J$ is that, as $R_S > R_0$, the voltage in the tip-sample junction collapses at small tip-sample distances, as can be seen in Fig. 1(c). The effect of this diminishing voltage bias $V_J$ is that the magnitude of the attractive electrostatic force does not keep increasing as the tip-sample distance is decreased, but instead decreases to zero, as shown in Fig. 1(d). In cases where the electrostatic force is the dominant force between tip and sample, that is, when it is greater than the van der Waals force and the tip is too far from the surface for chemical bonds to dominate the total tip-sample force, this decrease of magnitude of the electrostatic force can lead to positive values of $\Delta f$.

In order to investigate this, we acquired Kelvin parabolae over the Si(111)–$7 \times 7$ surface as a function of distance to the surface, and compared it to the mathematical model described above. Experiments were performed in an Omicron LT SPM system at a temperature of 4.4 K. Sensors were used with a spring constant $k = 1800\,\mathrm{Nm}^{-1}$ and nominal bulk tungsten tips. FM-AFM data were collected with the amplitude of oscillation set to 50 pm. As this amplitude is small compared to the tip-sample distances (which we comment upon later), we use Eq. (1) and approximate $k_{ts}$ by $\langle k_{ts} \rangle$. Reported current $I$ is an averaged current and biases refer to the sample with respect to the tip. Si(111)–$7 \times 7$ was prepared with several flash and anneal cycles.

Figs. 2(a) and 2(b), respectively, show AFM and STM data in constant height mode of the $7 \times 7$ surface. The similarity between the two images, and especially that the adatoms in the AFM data appear repulsive, indicates that these data are collected where the AFM resolution is dominated by the Phantom force. Based on previous measurements, we estimate that we are approximately 300 pm away from the point in which chemical contrast would dominate the image, that is, where chemical bonds between the tip and sample start to form.[2]

Taking this point as $z = 0$ pm, we retracted the tip up to 900 pm away from the surface and acquired $\Delta f(V_B)$ data. For several distances from the surface, the curves are shown in Fig. 2(c). Raw data are the solid lines that have been offset to clearly show their shape.

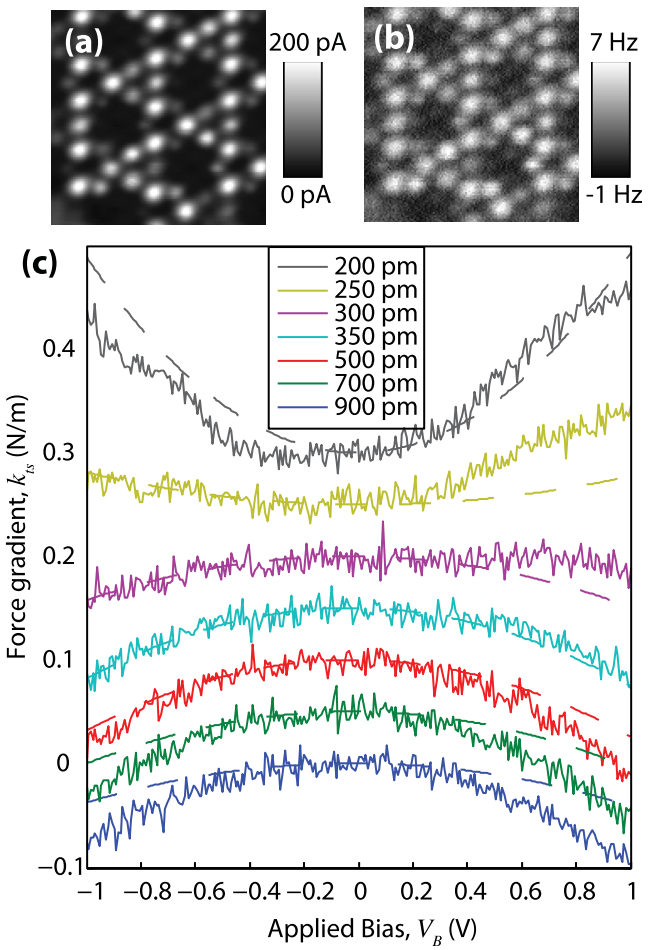


FIG. 2. (a) STM data taken at −1 V. (b) Simultaneous AFM data. (c) $k_{ts}$ versus $V_B$ sweeps taken various offset distances from the height of the images in (a) and (b).

When the tip is further from the surface, that is, $z \geq 500$ pm, the data appear as expected. The curves appear parabolic with negative curvature. However, as the tip further approaches the surface, the curves appear to flatten out and by a distance of $z = 250$ pm, the curves have a positive curvature.

We applied our model to these data to explain the upward curve as the tip approached the surface. An additional parameter, $z_0$, accounts for the unknown $z$-offset from the surface. For each curve, the only force that should change as a function of bias is the electrostatic force. Thus, by allowing an arbitrary offset, we can use a bounded least-squares algorithm and fit the parameters of $k_{ts}^{es}$. In this model, $R_S$ and $R_0$ cannot be independently determined, instead only their ratio can be determined by the fit. The best model outputs are shown in Fig. 2(c).

There is strong agreement between this proposed model and our $\Delta f$ data, especially for smaller $z$ values. As well as this spherical tip model, we also explored a parallel-plate model of tip-sample capacitance and found this agreement between data and model to be worse. The improvement with this spherical tip model indicates that with a more accurate tip model, agreement between data and the model could be improved. While we could increase the complexity of the tip model to better fit the data, for example, by incorporating a macroscopic shape that could improve the agreement at larger tip-sample distances, this model retains its simplicity while being able to show the most important feature, which is a change of sign of curvature at smaller $z$ values. The model does not incorporate the electronic structure of either the tip or the sample, treating both as ohmic devices, however, this appears valid within this distance regime as the simultaneously acquired $I(V_B)$ data did not yield any strong features. Furthermore, the values used for this fit are all reasonable: $\mathcal{R} = 4.0\,\mathrm{nm}, R_S/R_0 = 1.24 \times 10^6, z_0 = 700\,\mathrm{pm}, \kappa = 0.9 \times 10^{10}\,\mathrm{m}^{-1}$, and $V_{CPD} = 0.021\,\mathrm{V}$.

We can compare the model value of $\kappa$ to that from corresponding $I(z)$ spectra collected at various biases. At both positive and negative biases, $I(z)$ spectra yield a value of $1 \times 10^{10}\,\mathrm{m}^{-1}$, which is very close to the model parameter.

The current collected in the bias sweeps can be used to determine values for both $R_0$ and $R_S$. Assuming that the tunneling current is $V_B/(R_S + R_0\, e^{2\kappa z})$, we can use the current and the fitted value of $R_S/R_0$. At $z = 200$ pm and $V_B = 1$ V, $I = 4$ pA. This would yield values of $R_0 = 21\,\mathrm{k\Omega}$ and $R_S = 26\,\mathrm{G\Omega}$. The contact resistance $R_0$ is higher is higher than the value of $1/G_0$, but this is a metal-semiconductor contact in which the metallic tip had been conditioned by repeated pokes into the surface.

We have reported a model for KPFM that incorporates the Phantom force. This model can explain Kelvin parabola with positive curvature. It is also another explanation for a drop in the exponential character of the tunneling current, as has been previously reported.[19] While it might be surprising that a model based upon a Drude approximation should be so accurate given the quantum nature of the tip-sample junction, the accuracy of Ohm's law at the atomic scale has been recently reported with careful transport measurements.[20]

We would like to thank T. Hofmann and T. Wutscher for their help with the experimental setup. Financial support from the Deutsche Forschungsgemeinschaft (GRK 1570) is kindly acknowledged.

[1]M. Nonnenmacher, M. P. OBoyle, and H. K. Wickramasinghe, Appl. Phys. Lett. **58**, 2921 (1991).
[2]A. J. Weymouth, T. Wutscher, J. Welker, T. Hofmann, and F. Giessibl, Phys. Rev. Lett. **106**, 226801 (2011).
[3]T. Wutscher, A. Weymouth, and F. Giessibl, Phys. Rev. B **85**, 195426 (2012).
[4]A. Sadeghi, A. Baratoff, S. Ghasemi, S. Goedecker, T. Glatzel, S. Kawai, and E. Meyer, Phys. Rev. B **86**, 075407 (2012).
[5]C. Barth and C. R. Henry, Nanotechnology **17**, S155 (2006).
[6]L. Nony, A. Foster, F. Bocquet, and C. Loppacher, Phys. Rev. Lett. **103**, 036802 (2009).
[7]L. Gross, F. Mohn, P. Liljeroth, J. Repp, F. J. Giessibl, and G. Meyer, Science **324**, 1428 (2009).
[8]F. Mohn, L. Gross, N. Moll, and G. Meyer, Nat. Nanotechnol. **7**, 227 (2012).
[9]F. Bocquet, L. Nony, and C. Loppacher, Phys. Rev. B **83**, 035411 (2011).
[10]Y. Rosenwaks, R. Shikler, T. Glatzel, and S. Sadewasser, Phys. Rev. B **70**, 085320 (2004).
[11]S. Sadewasser, P. Jelínek, C.-K. Fang, O. Custance, Y. Yamada, Y. Sugimoto, M. Abe, and S. Morita, Phys. Rev. Lett. **103**, 266103 (2009).
[12]T. R. Albrecht, P. Grütter, D. Horne, and D. Rugar, J. Appl. Phys. **69**, 668 (1991).
[13]F. J. Giessibl, Rev. Mod. Phys. **75**, 949 (2003).
[14]S. Modesti, H. Gutzmann, J. Wiebe, and R. Wiesendanger, Phys. Rev. B **80**, 125326 (2009).
[15]K.-i. Morita, Y. Sugimoto, M. Abe, and S. Morita, Appl. Phys. Express **4**, 115201 (2011).
[16]Y. Sugimoto, K. Ueda, M. Abe, and S. Morita, J. Phys.: Condens. Matter **24**, 084008 (2012).
[17]S. Hudlet, M. Saint Jean, C. Guthmann, and J. Berger, Eur. Phys. J. B **2**, 5 (1998).
[18]P. Jelínek, M. Švec, P. Pou, R. Perez, and V. Cháb, Phys. Rev. Lett. **101**, 176101 (2008).
[19]Y. Sugimoto, Y. Nakajima, D. Sawada, K. Morita, M. Abe, and S. Morita, Phys. Rev. B **81**, 245322 (2010).
[20]B. Weber, S. Mahapatra, H. Ryu, S. Lee, A. Fuhrer, T. C. G. Reusch, D. L. Thompson, W. C. T. Lee, G. Klimeck, L. C. L. Hollenberg, and M. Y. Simmons, Science **335**, 64 (2012).